Onset of Partonic Collectivity in Heavy-Ion Collisions at RHIC

The STAR Collaboration
(Dated: January 5, 2025)

Partonic collectivity is one of the necessary signatures for the formation of quark-gluon-plasma in high-energy nuclear collisions. Number of constituent quarks (NCQ) scaling has been observed for light hadron elliptic flow v_2 in top energy nuclear collisions at RHIC and the LHC, presenting the partonic collectivity. In this letter, a systematic analysis of v_2 of $\pi^{\pm}$, $K^{\pm}$, K_S^0, p and Λ in Au+Au collisions at $\sqrt{s_{\rm NN}}$ = 3.2, 3.5, 3.9, and 4.5 GeV, with the STAR experiment at RHIC, is presented. NCQ scaling is markedly violated at 3.2 GeV, reflecting a hadronic-interaction dominated equation of state. However, as the collision energy increases to 4.5 GeV in Au+Au systems, a gradual restoration of the scaling is observed. This breakdown and subsequent restoration of NCQ scaling provides evidence for the onset of partonic interactions in these collisions. The energy dependence of the scaling is discussed within the framework of transport model calculations.

Elliptic flow (v_2), the second-order harmonic coefficient in the Fourier expansion of the final state particle azimuthal distribution with respect to the reaction plane, is sensitive to constituent interactions and the degrees of freedom of the created matter in heavy-ion collisions [1]. The significant v_2 signal and the Number of Constituent Quarks (NCQ) scaling are considered as evidence of quark-gluon-plasma (QGP) formation in high-energy relativistic heavy-ion collisions [2–6]. NCQ scaling refers to the observation that particle v_2 collapses onto a universal curve when scaled by the number of constituent quarks, indicating the presence of quark degrees of freedom in the medium. As the collision energy gradually decreases to a certain threshold, the high temperature and energy density conditions necessary for the formation of QGP will no longer be satisfied. Consequently, such experimental signals on elliptic flow are expected to disappear. The Beam Energy Scan (BES) at the Brookhaven Relativistic Heavy Ion Collider (RHIC) aims to explore the Quantum Chromodynamics (QCD) phase structure by lowering the collision energy, spanning an energy range from $\sqrt{s_{\rm NN}}$ = 3 to 62.4 GeV, in search of possible signals for a QCD first-oder phase boundary and critical point through heavy-ion collision experiments. [7–10].

In the elliptic flow measurements of the first phase of RHIC beam energy scan (BES-I), we observed a relatively good agreement of NCQ scaling in collisions with $\sqrt{s_{\rm NN}} \geq$ 7.7 GeV [11–14]. Additionally, observations of a possible deviation from NCQ scaling, around 2σ, were noted for the ϕ meson v_2 in collisions at $\sqrt{s_{\rm NN}}$ = 7.7 GeV and 11.5 GeV [11–14]. Further investigation with larger data samples is warranted. However, the latest published elliptic flow results from the STAR experiment at $\sqrt{s_{\rm NN}}$ = 3 GeV show that at this energy, NCQ scaling breaks among π^+, K^+ and proton v_2 [15]. The second phase of the RHIC beam energy scan (BES-II) focuses on energies ranging from $\sqrt{s_{\rm NN}}$ = 3 to 19.6 GeV, corresponding to a baryon chemical potential range of 750 to 205 MeV [16–18]. STAR has conducted a series of detector upgrades for BES-II: inner Time Projection Chamber (iTPC) to improve the track quality [19]; endcap Time of Flight (eTOF) to enhance the identification capability in the mid-rapidity region; Event Plane Detector (EPD) to measure the collision centrality and the event plane of the collision event [20].

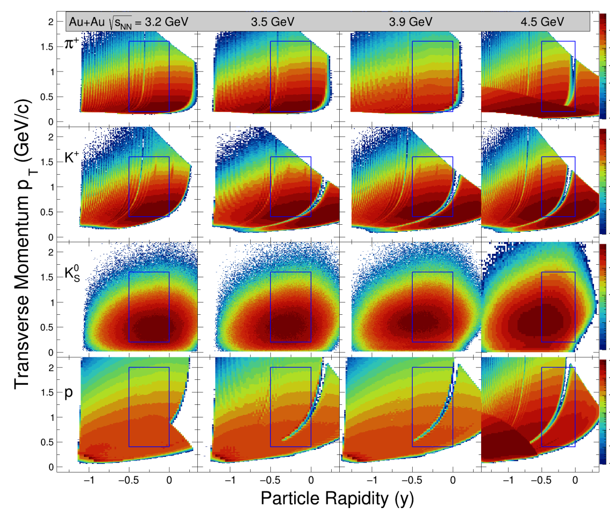

FIG. 1. The transverse momentum (p_T) and identified particle rapidity (y) distribution for π^+, K^+, K_S^0, p from Au+Au collisions at $\sqrt{s_{\rm NN}}$ = 3.2, 3.5, 3.9, and 4.5 GeV. The blue boxes represent the acceptance ($-0.5 < y < 0$) used for elliptic flow measurements.

In this letter, we report v_2 measurements for $\pi^{\pm}$, $K^{\pm}$, K_S^0, p, and Λ in Au+Au collisions at $\sqrt{s_{\rm NN}}$ = 3.2, 3.5, 3.9, and 4.5 GeV. These data were collected in 2019 and 2020 during the STAR fixed-target (FXT) program at RHIC. Datasets for collision energies above 4.5 GeV in the FXT mode are not included due to limited mid-rapidity coverage. The results presented here are analyzed from minimum bias events of Au+Au collisions. The primary vertex position of each event along the beam direction is selected to be within 198 to 202 cm from the center of the Time Projection Chamber (TPC). Additionally, the vertex along the radial direction is chosen to be smaller than 2 cm to eliminate possible beam interactions with

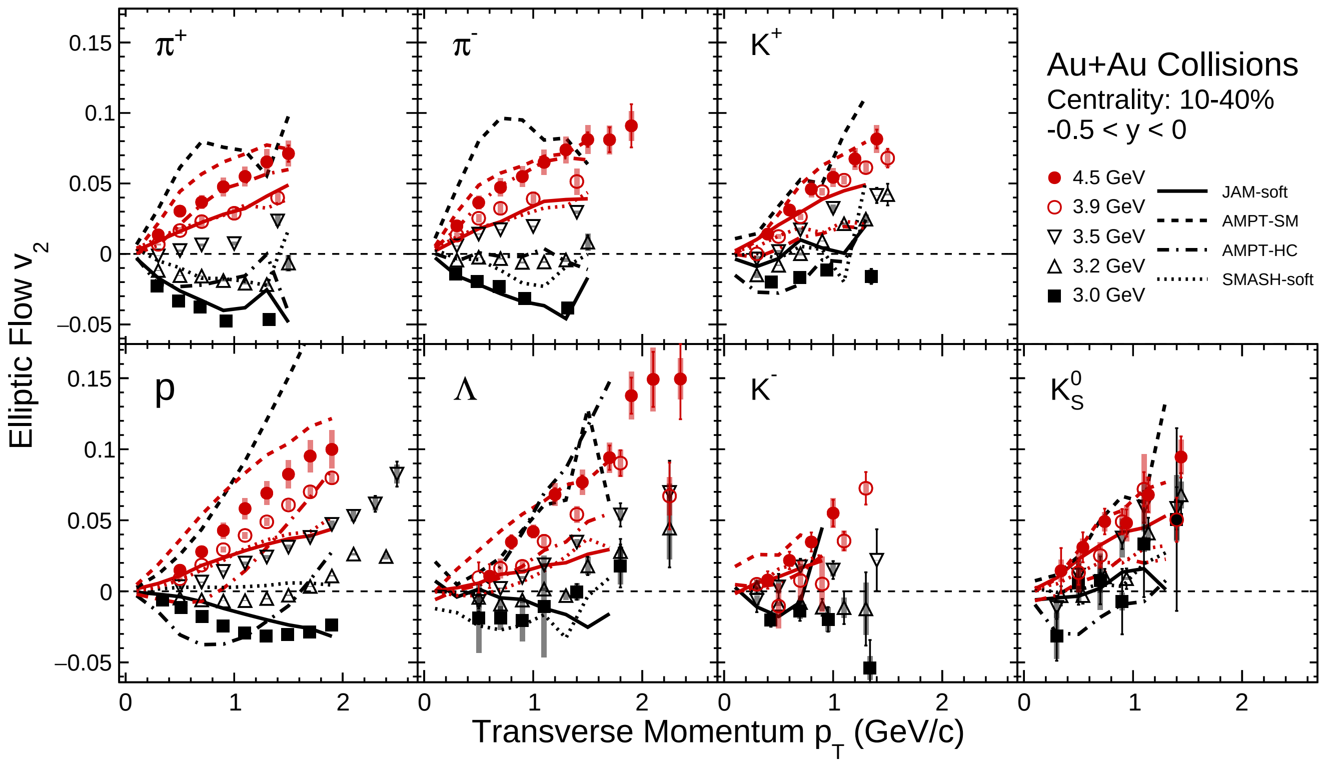

FIG. 2. Transverse momentum (p_T) dependence of v_2 for $\pi^{\pm}, K^{\pm}, K^0_S, p, \Lambda$ in 10-40% centrality for Au+Au collisions at $\sqrt{s_{\rm NN}}$ = 3.0, 3.2, 3.5, 3.9, and 4.5 GeV. Statistical and systematic uncertainties are shown as bars and bands, respectively. Different lines represent the results from JAM-soft (solid), AMPT-SM (dashed), AMPT-HC (dash-dotted), and SMASH-soft (dotted) calculations: ~~orange~~ red for 4.5 GeV, and ~~blue~~ black for 3.0 GeV. For clarity, the error bars of the model calculations are not shown, and K^- calculations for 3.0 GeV from AMPT and SMASH are not shown due to the rarity of production.

the vacuum pipe. To select high-quality tracks, we require a distance of closest approach (DCA) from the vertex of DCA $\leq$ 3 cm and a minimum of 15 space points within the acceptance of the TPC. Runs where the mean value of one or more physics variables exceeds 5 times the standard deviation across all runs are labeled as bad runs and excluded from the analysis. Pileup events, resulting from the limited temporal and spatial resolution of the TPC in recognizing multiple events as a single event, are removed by correlating the TPC multiplicity with the Time of Flight (TOF) matched multiplicity. Collision centralities are determined by fitting the measured charged particle multiplicities from the TPC with a Monte Carlo Glauber model. For particle identification (PID) of $\pi^{\pm}, K^{\pm}$, and p, a combination of the TPC and the TOF detector is used, which relies on the ionization energy loss information and time-of-flight information, respectively. A minimum identification purity of $> 90\%$ is required for elliptic flow measurements, with the PID contamination effect estimated as a systematic uncertainty. The strange hadrons K^0_S and Λ are reconstructed by pairing their daughter tracks via the Kalman Filter (KF) particle package [21, 22].

The transverse momentum (p_T) and rapidity (y) distributions of identified particles π^+, K^+, K^0_S, and p from Au+Au collisions at $\sqrt{s_{\rm NN}}$ = 3.2, 3.5, 3.9, and 4.5 GeV are shown in Fig. 1. The blue boxes show the calculation region ($-0.5 < y < 0$) for elliptic flow measurements. Due to the asymmetry of the phase space acceptance in fixed-target collisions, the 3-sub event method is applied to reconstruct the event plane and estimate the event plane resolution [23]:

$$\langle \cos\left[n\left(\Psi^a_m - \Psi_r\right)\right]\rangle = \sqrt{\frac{\langle \cos\left[n\left(\Psi^a_m - \Psi^b_m\right)\right]\rangle \langle \cos\left[n\left(\Psi^a_m - \Psi^c_m\right)\right]\rangle}{\langle \cos\left[n\left(\Psi^b_m - \Psi^c_m\right)\right]\rangle}} \quad (1)$$

where Ψ_r represents the reaction plane, n denotes the corresponding Fourier coefficient v_n, and m indicates the m-th order harmonic event plane, Ψ^a_m, Ψ^b_m, and Ψ^c_m represent the three sub-event planes. As the first-order coefficient (v_1) is more significant than v_2 within this energy region, v_2 is measured with respect to the first-order event plane, with resolution R_{12} about 19-24% in mid-central 10-40% collisions. The p_T dependence of v_2 measurements considers the detector efficiency as a function of transverse momentum p_T and rapidity y. This efficiency encompasses the track efficiency of the TPC

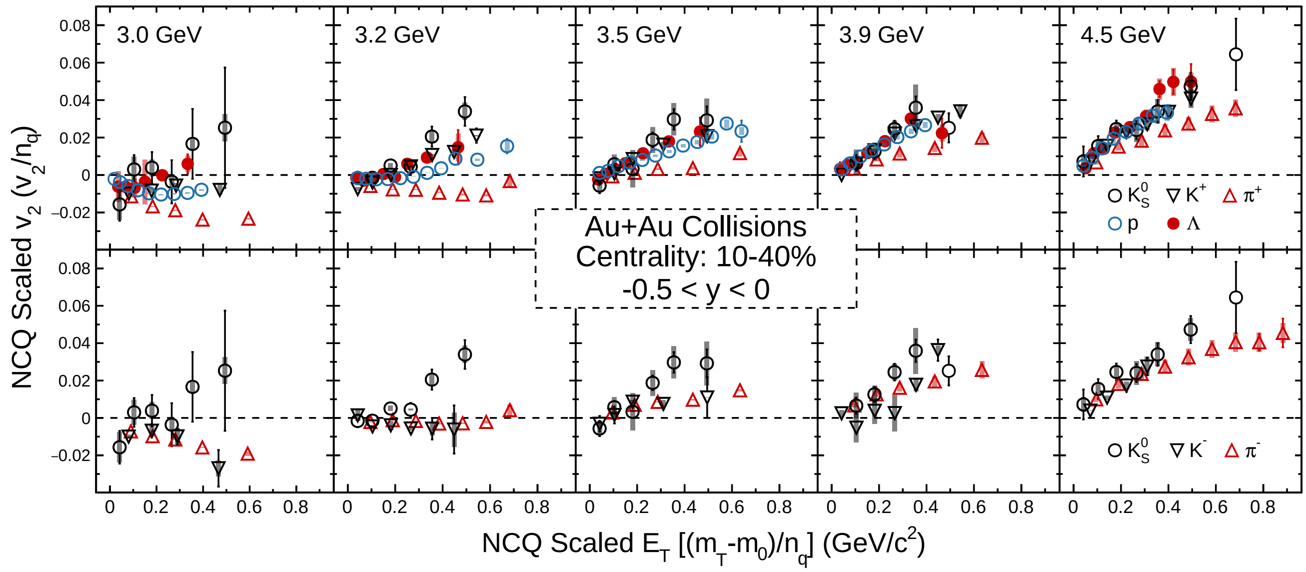

FIG. 3. The number of constituent quarks n_q scaled v_2 as a function of n_q scaled E_T $(m_T - m_0)$ for particles (upper panel) and anti-particles (lower panel) in 10-40% centrality for Au+Au collisions at $\sqrt{s_{\rm NN}}$ = 3.0, 3.2, 3.5, 3.9, and 4.5 GeV. Statistical and systematic uncertainties are shown as bars and bands, respectively.

and the TOF matching efficiency for $\pi^\pm$, $K^\pm$, and p, as well as the additional reconstruction efficiency for K^0_S and Λ. These efficiencies are estimated using the embedding method within the STAR analysis framework. The systematic uncertainties in the measurements are determined by varying the analysis cuts mentioned above, which include track quality cuts, particle identification cuts, and event plane resolution. For each cut variable, we assign the maximum deviation from the default value as the systematic error originating from that source. Assuming these sources are uncorrelated, the total systematic uncertainty is calculated by summing them together quadratically. The largest systematic uncertainty in proton v_2 at 4.5 GeV, arising from event plane resolution, is less than 13.3%. The systematic uncertainty from particle identification cuts is less than 1.5%, and less than 1.7% for track quality cuts.

Figure 2 presents the p_T dependence of v_2 for $\pi^\pm, K^\pm, K^0_S, p, \Lambda$ in 10-40% centrality for Au+Au collisions at $\sqrt{s_{\rm NN}}$ = 3.0, 3.2, 3.5, 3.9, and 4.5 GeV. The data at 3.2, 3.5, 3.9, and 4.5 GeV represent new measurements, while the 3.0 GeV data is taken from a previous publication [15]. Due to the rarity of anti-protons and $\bar{\Lambda}$ in this collision energy range, measurements of the elliptic flow for these two particles are not available. Clear energy dependence of v_2 is observed for each particle species. In lower energy collisions, the passing time ($\sim 2R/\gamma\beta$) of the projectile and target spectators is comparable to the mean time of particle freeze-out. As a result, the in-plane expansion is hindered by the spectators, a phenomenon known as the shadowing effect. Particles are preferentially emitted in the direction perpendicular to the reaction plane, leading to a negative signal. The v_2 as a function of p_T changes from negative to positive between 3.0 GeV and 4.5 GeV, indicating that the spectator-shadowing effect decreases rapidly within this energy range. The calculations from the Jet AA Microscopic Transport Model (JAM) [24, 25], Multi-Phase Transport Model: Hadron Cascade (AMPT-HC) and String Melting (AMPT-SM) mode [26, 27], and Simulating Many Accelerated Strongly interacting Hadrons (SMASH) [28] are represented by the lines. For the lowest collsion energy 3 GeV, the hadronic transport models JAM, AMPT-HC, and SMASH qualitatively describe the v_2 data. The multi-phase transport model AMPT-SM (~~blue~~ black dashed line) predicts the opposite sign of v_2, which could be due to the spectator-shadowing effect is not properly taken into account. For 4.5 GeV, the hadronic transport models generally underestimate the v_2 data (except $\pi^\pm$ from AMPT-HC); in contrast, AMPT-SM mode better describes the v_2 data. This suggests that parton interactions play an important role in generating such a significant v_2 signal.

The NCQ scaling is expected to reflect the effective degrees of freedom of the medium. Figure 3 represents the number of constituent quarks n_q scaled v_2 as a function of n_q scaled E_T $(m_T - m_0)$ for particles and ~~antiparticles~~ anti-particles separately in 10-40% centrality for Au+Au collisions at $\sqrt{s_{\rm NN}}$ = 3.0, 3.2, 3.5, 3.9, and 4.5 GeV. In collisions at 3.0 and 3.2 GeV, it can be clearly observed that the NCQ scaling is broken, with each particle exhibiting a different trend. As the collision energy increases from 3.2 to 4.5 GeV, the NCQ scaling gradually improves. These observations suggest that hadronic interactions dominate

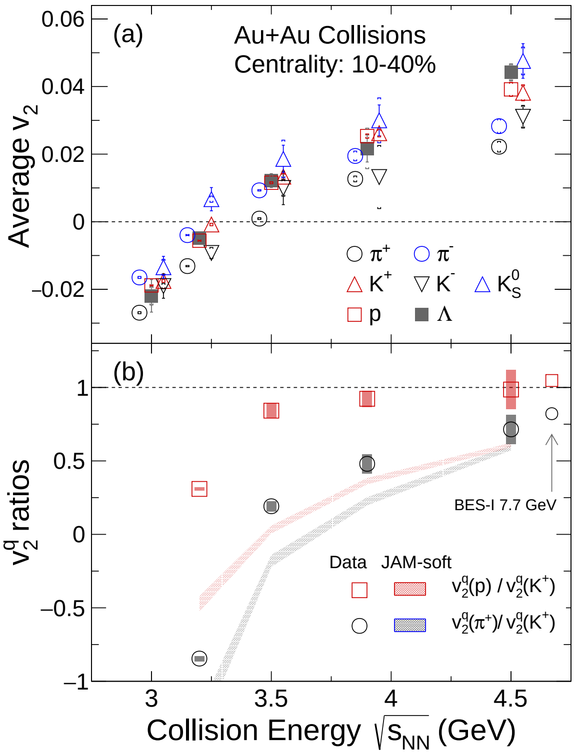

FIG. 4. (a): The energy dependence of p_T integrated v_2 for $\pi^\pm, K^\pm, K^0_S, p, \Lambda$ in 10-40% centrality from Au+Au collisions at $\sqrt{s_{\rm NN}}$ = 3.0, 3.2, 3.5, 3.9, and 4.5 GeV. For clarity, the X-axis values of pions and kaons are shifted by ±0.05 respectively. (b): The energy dependence of ~~NCQ~~ n_q scaled v_2 ratios ~~for $\pi^+/K^+, p/K^+$~~ of $v_2^q(\pi^+)/v_2^q(K^+)$ and $v_2^q(p)/v_2^q(K^+)$ at $E_T/n_q = 0.4$ GeV/c^2 in the same centrality~~and energies~~. Statistical and systematic uncertainties are shown as bars and bands, respectively. The JAM calculations with baryonic mean field are shown as color bands~~: grey for π^+/K^+, red for p/K^+~~.

the equation of state of the created matter at 3.0 and 3.2 GeV, while partonic interactions become more important at collision energies greater than 3.2 GeV. On the model side, JAM model better describes the NCQ breaking at 3.0 GeV but fails to capture the scaling behavior at 4.5 GeV; AMPT-SM shows better scaling behavior than other hadronic transport models at 4.5 GeV. It's worth noting that π^+ always deviates from the scaling and is smaller than other particles at each energy. The p_T/n_q scaling exhibits better performance than $(m_T - m_0)/n_q$ for π^+, suggesting that the observed deviation in π^+ is primarily attributed to the significantly smaller mass of pions compared to other hadrons.

We further investigate the p_T integrated v_2 as a function of collision energy. Figure 4 (a) shows the energy dependence of p_T integrated v_2 for $\pi^\pm$, $K^\pm$, K^0_S, protons, Λ in 10-40% centrality from Au+Au collisions at $\sqrt{s_{\rm NN}}$ = 3.0, 3.2, 3.5, 3.9, and 4.5 GeV. The integrated v_2 is calculated within $0.2 < p_T(\mathrm{GeV}/c) < 1.6$ for $\pi^\pm$, $0.4 < p_T(\mathrm{GeV}/c) < 1.6$ for $K^\pm, K^0_S$, $0.4 < p_T(\mathrm{GeV}/c) < 2.0$ for p, Λ. p_T integrated v_2 changes from negative to positive from 3.0 ~~GeV~~ to 4.5 GeV, crossing zero at about 3.2 GeV. Clear differences between π^- and π^+ are observed at each energy, and the differences become smaller as the energy increases. This is consistent with the picture of the baryon number transport — quarks transported from beam rapidity to mid-rapidity experience more violent scatterings than quarks produced at mid-rapidity. Additionally, the initial nuclear matter is a neutron-rich environment, causing a larger transported effect for $\pi^-(\bar{u}d)$ compared to $\pi^+(u\bar{d})$ [29]. Although the uncertainties are large for $K^\pm, K^0_S$, these three kaons exhibit ordering behavior, i.e., $K^0_S(d\bar{s}) > K^+(u\bar{s}) > K^-(\bar{u}s)$, which is also consistent with the transported effect. On the other side, the v_2 of protons and Λ are consistent within statistical uncertainties.

In order to quantify the trend of NCQ scaling with collision energy, Fig. 4 (b) shows the ~~NCQ~~ n_q scaled v_2 ~~ratio of π^+/K^+ and p/K^+ as a function of collision energy~~ ratios of $v_2^q(\pi^+)/v_2^q(K^+)$ and $v_2^q(p)/v_2^q(K^+)$ at E_T/n_q = 0.4 GeV/c^2 ~~. The NCQ scaling ratio of p/K^+~~ as a function of collision energy, where the v_2^q represents the n_q scaled v_2 (v_2/n_q). The ratio of $v_2^q(p)/v_2^q(K^+)$ is close to unity at 3.9 and 4.5 GeV, while it deviates significantly at 3.2 GeV. Although hadronic model ~~(JAM)~~ JAM calculations fit the $v_2(p_T)$ data better at lower collision energies, they underestimate the ratios throughout the energy range studied.

In summary, we present the elliptic flow of identified hadrons $\pi^\pm$, $K^\pm$, K^0_S, p, Λ in Au+Au collisions at $\sqrt{s_{\rm NN}}$ = 3.2, 3.5, 3.9, and 4.5 GeV. The v_2 of these particles changes from negative to positive around 3.2 GeV. At the lower colliding energy, $\sqrt{s_{\rm NN}} \leq 3.2$ GeV, NCQ scaling breaks down and the calculations from the hadronic transport model JAM [24, 25] reproduce the transverse momentum dependence of the measured $v_2(p_T)$, implying hadronic interaction dominance. As collision energy increases, a gradual restoration of NCQ scaling is observed, and the hadronic transport model underpredicts, while the multi-phase transport model more accurately captures the collectivity observed in the 4.5 GeV data. The observed breakdown and subsequent restoration of NCQ scaling suggest an increasing significance of partonic interactions in collisions at $\sqrt{s_{\rm NN}} \geq$ ~~3.5~~ 4.5 GeV, signaling the emergence of partonic collectivity.

Acknowledgments: We thank the RHIC Operations Group and RCF at BNL, the NERSC Center at LBNL, and the Open Science Grid consortium for providing resources and support. This work was supported in part by the Office of Nuclear Physics within the U.S. DOE Office of Science, the U.S. National Science Foundation, National Natural Science Foundation of China, Chinese Academy of Science, the Ministry of Science and Technology of China and the Chinese Ministry of Education, the Higher Education Sprout Project by Ministry of Education at NCKU, the National Research Foundation of Korea, Czech Science Foundation and Ministry of Education, Youth and Sports of the Czech Republic, Hungarian National Research, Development and Innovation Office, New National Excellency Programme of the Hungarian Ministry of Human Capacities, Department of Atomic Energy and Department of Science and Technology of the Government of India, the National Science Centre of Poland, the Ministry of Science, Education and Sports of the Republic of Croatia, German Bundesministerium für Bildung, Wissenschaft, Forschung and Technologie (BMBF), Helmholtz Association, Ministry of Education, Culture, Sports, Science, and Technology (MEXT) and Japan Society for the Promotion of Science (JSPS).

---

[1] S. A. Voloshin, A. M. Poskanzer, and R. Snellings, Landolt-Bornstein **23**, 293 (2010).
[2] J. Adams *et al.* (STAR), Nucl. Phys. A **757**, 102 (2005).
[3] K. Adcox *et al.* (PHENIX), Nucl. Phys. A **757**, 184 (2005), arXiv:nucl-ex/0410003.
[4] L. Adamczyk *et al.* (STAR), Phys. Rev. Lett. **116**, 062301 (2016).
[5] L. Adamczyk *et al.* (STAR), Phys. Rev. Lett. **118**, 212301 (2017).
[6] P. Braun-Munzinger and J. Stachel, Nature **448**, 302 (2007).
[7] K. Fukushima and T. Hatsuda, Rept. Prog. Phys. **74**, 014001 (2011).
[8] A. Bzdak, S. Esumi, V. Koch, J. Liao, M. Stephanov, and N. Xu, Phys. Rept. **853**, 1 (2020), arXiv:1906.00936 [nucl-th].
[9] X. Luo, S. Shi, N. Xu, and Y. Zhang, Particles **3**, 278 (2020).
[10] J.-H. Chen, X. Dong, X.-H. He, H.-Z. Huang, F. Liu, X.-F. Luo, Y.-G. Ma, L.-J. Ruan, M. Shao, S.-S. Shi, X. Sun, A.-H. Tang, Z.-B. Tang, F.-Q. Wang, H. Wang, Y. Wang, Z.-G. Xiao, G.-N. Xie, N. Xu, Q.-H. Xu, Z.-B. Xu, C. Yang, S. Yang, W.-M. Zha, Y.-P. Zhang, Y.-F. Zhang, J. Zhao, and X.-L. Zhu, Nuclear Science and Techniques **35**, 214 (2024).
[11] L. Adamczyk *et al.* (STAR), Phys. Rev. Lett. **110**, 142301 (2013), arXiv:1301.2347 [nucl-ex].
[12] L. Adamczyk *et al.* (STAR), Phys. Rev. C **88**, 014902 (2013), arXiv:1301.2348 [nucl-ex].
[13] L. Adamczyk *et al.* (STAR), Phys. Rev. C **93**, 014907 (2016), arXiv:1509.08397 [nucl-ex].
[14] L. Adamczyk *et al.* (STAR), Phys. Rev. C **86**, 054908 (2012), arXiv:1206.5528 [nucl-ex].
[15] M. S. Abdallah *et al.* (STAR), Phys. Lett. B **827**, 137003 (2022), arXiv:2108.00908 [nucl-ex].
[16] J. Cleymans, H. Oeschler, K. Redlich, and S. Wheaton, Phys. Rev. C **73**, 034905 (2006), arXiv:hep-ph/0511094.
[17] A. Andronic, P. Braun-Munzinger, and J. Stachel, Nucl. Phys. A **772**, 167 (2006), arXiv:nucl-th/0511071.
[18] L. Adamczyk *et al.* (STAR), Phys. Rev. C **96**, 044904 (2017), arXiv:1701.07065 [nucl-ex].
[19] C. Yang (STAR), Nucl. Phys. A **967**, 800 (2017).
[20] J. Adams *et al.*, Nucl. Instrum. Meth. A **968**, 163970 (2020), arXiv:1912.05243 [physics.ins-det].
[21] I. Kisel (CBM), J. Phys. Conf. Ser. **1070**, 012015 (2018).
[22] A. Banerjee, I. Kisel, and M. Zyzak, Int. J. Mod. Phys. A **35**, 2043003 (2020).
[23] A. M. Poskanzer and S. A. Voloshin, Phys. Rev. C **58**, 1671 (1998).
[24] Y. Nara and A. Ohnishi, Phys. Rev. C **105**, 014911 (2022), arXiv:2109.07594 [nucl-th].
[25] Y. Nara, A. Jinno, K. Murase, and A. Ohnishi, Phys. Rev. C **106**, 044902 (2022), arXiv:2208.01297 [nucl-th].
[26] Z.-W. Lin, C. M. Ko, B.-A. Li, B. Zhang, and S. Pal, Phys. Rev. C **72**, 064901 (2005).
[27] G.-C. Yong, Phys. Lett. B **848**, 138327 (2024), arXiv:2306.16005 [nucl-th].
[28] J. Weil *et al.* (SMASH), Phys. Rev. C **94**, 054905 (2016), arXiv:1606.06642 [nucl-th].
[29] J. C. Dunlop, M. A. Lisa, and P. Sorensen, Phys. Rev. C **84**, 044914 (2011), arXiv:1107.3078 [hep-ph].